Brain Research Bulletin 121 (2016) 26–41

Contents lists available at ScienceDirect

Brain Research Bulletin

journal homepage: www.elsevier.com/locate/brainresbull

Research report

Cognitive stimulation of the default-mode network modulates functional connectivity in healthy aging

Matteo De Marco[a,b], Francesca Meneghello[a], Davide Duzzi[a,c], Jessica Rigon[a], Cristina Pilosio[a], Annalena Venneri[a,b,*]

[a] IRCCS Fondazione Ospedale San Camillo, Venice, Italy
[b] Department of Neuroscience, University of Sheffield, Sheffield, UK
[c] Department of Biomedical Sciences, Metabolic and Neuroscience, University of Modena and Reggio Emilia, Modena, Italy

ARTICLE INFO

Article history:
Received 2 September 2015
Received in revised form 3 November 2015
Accepted 4 December 2015
Available online 11 December 2015

Keywords:
Alzheimer's disease
Brain networks
Resting state
fMRI
Mild cognitive impairment

ABSTRACT

A cognitive-stimulation tool was created to regulate functional connectivity within the brain Default-Mode Network (DMN). Computerized exercises were designed based on the hypothesis that repeated task-dependent coactivation of multiple DMN regions would translate into regulation of resting-state network connectivity.

Forty seniors (mean age: 65.90 years; SD: 8.53) were recruited and assigned either to an experimental group ($n = 21$) who received one month of intensive cognitive stimulation, or to a control group ($n = 19$) who maintained a regime of daily-life activities explicitly focused on social interactions. An MRI protocol and a battery of neuropsychological tests were administered at baseline and at the end of the study. Changes in the DMN (measured via functional connectivity of posterior-cingulate seeds), in brain volumes, and in cognitive performance were measured with mixed models assessing group-by-timepoint interactions. Moreover, regression models were run to test gray-matter correlates of the various stimulation tasks.

Significant associations were found between task performance and gray-matter volume of multiple DMN core regions. Training-dependent up-regulation of functional connectivity was found in the posterior DMN component. This interaction was driven by a pattern of increased connectivity in the training group, while little or no up-regulation was seen in the control group. Minimal changes in brain volumes were found, but there was no change in cognitive performance.

The training-dependent regulation of functional connectivity within the posterior DMN component suggests that this stimulation program might exert a beneficial impact in the prevention and treatment of early AD neurodegeneration, in which this neurofunctional pathway is progressively affected by the disease.

1. Introduction

A specific pattern of change in brain function is observed when individuals disengage from attending to overt cognitive tasks and are "at rest" (Greicius et al., 2003). During this mental state the brain is free to engage in undisturbed, spontaneous, "self-projecting" cognitive computations, such as autobiographical remembering, envisioning of the future, theory of mind, or spatial navigation imagery (Buckner and Carroll, 2007). The circuit of areas showing increased activity during these states was labelled Default Mode Network (DMN) (Raichle et al., 2001) and includes the posterior cingulate cortex, the medial prefrontal cortex, the inferior parietal lobule, the lateral temporal cortex, and the hippocampal formation (Buckner et al., 2008). The precuneus has also been recognized by some authors as part of the DMN (Utevsky et al., 2014), as well as a midline cerebellar lobule (Habas et al., 2009). Statistical evidence has demonstrated that this network is not a unitary entity, but is most likely the combination of distinct sub-systems. Andrews-Hanna et al. (2010) used graph-analytical techniques and clustering analysis and were able to assign the various hubs of the DMN to a core kernel consisting of the posterior cingulate and the anterior medial prefrontal cortex, and to two sub-systems, one

* Corresponding author at: Department of Neuroscience—Medical School, University of Sheffield, Beech Hill Road, Royal Hallamshire Hospital, Sheffield S10 2RX, UK. Fax: +44 114 2222290.
E-mail address: a.venneri@sheffield.ac.uk (A. Venneri).

http://dx.doi.org/10.1016/j.brainresbull.2015.12.001
0361-9230/

encompassing the temporal hubs and the dorsomedial prefrontal cortex, and one including retrosplenial, ventromedial prefrontal, inferior parietal and mediotemporal cortices. This statistical separation appears to reflect a functional dissociation, as each of the two sub-systems was found to sustain its preferential set of spontaneous cognitive processes (Andrews-Hanna et al., 2010). The use of independent component analysis has then revealed the existence of another type of statistical dissociation. The DMN is very often estimated as two distinct components, namely an anterior and a posterior one (Uddin et al., 2009). Aside from its statistical properties, this sub-divison appears to be relevant in the description of neurodegeneration caused by Alzheimer's disease (AD). In fact, the evidence collected in some investigations suggests that, in clinically estabilished AD, the posterior DMN is pathologically down-regulated, while the anterior DMN is pathologically up-regulated (Damoiseaux et al., 2012; Jones et al., 2011). In addition to that, AD is associated with a progressive disconnection between the anterior and posterior hubs of the DMN. This has been found using independent component analysis (Song et al., 2013) and graph theory (Santz-Arigita et al., 2010), and it has also been suggested by the analysis of low frequency fluctuations in BOLD signal (Wang et al., 2007).

The hierarchical sub-division of the DMN into separate subsystems and the identification of the effects of AD on each sub-system is particularly relevant for the creation of preventive and therapeutic instruments. It has been suggested that the framework describing modifications in functional connectivity generated by AD could be an optimal model to develop and assess the efficacy of new pharmacological treatments (Hampel et al., 2011). At the moment, the most recognized form of pharmacological treatment in AD is based on the enhancement of cholinergic neurotransmission. Enhanced neurotransmission at a synaptic level should reflect regulation of circuital connectivity at a systemic level. Based on this principle, some teams investigated changes in connectivity within the DMN after treatment with donepezil (Solé-Padullés et al., 2013) and memantine (Lorenzi et al., 2011). In a similar way, it was recently suggested that even cognitive interventions for AD could be designed and assessed based on the DMN framework (De Marco et al., 2014).

It has been indicated that increased resting-state functional connectivity displayed by a set of areas would be the result of frequent co-activation of those areas during goal-directed brain function (Martínez et al., 2013). This principle would resemble the Hebbian paradigm "Neurons that fire together, wire together", not applied to single cells connections, but to a larger scale of multiple-neuron network (Cheng et al., 2012). Although a number of experimental trials have investigated the impact of cognitive stimulation on functional connectivity in healthy adults (e.g. Jolles et al., 2013; Martínez et al., 2013; Takeuchi et al., 2011a; Voss et al., 2012), no study has specifically tested a program of exercises, the conceptualization of which is focused on the DMN.

We created a set of computerized tasks with multiple cognitive demands to induce co-activation of different DMN regions. We then administered a 20-session protocol of these network-based tasks to elderly adults without cognitive impairment. We hypothesized that this program would up-regulate functional connectivity within the posterior DMN, and would also up-regulate connectivity between the anterior and posterior components. The main goal of the study was to test the efficacy of such model of intervention in healthy aging in order to justify its application in a clinical population with AD in its prodromal stage. The multi-dimensional process of healthy aging features decrease of functional connectivity within the DMN components in a qualitatively similar, yet non pathological form as that observed along the severity stages of AD (e.g. Jones et al., 2011; Koch et al., 2010; Mevel et al., 2013; Mowinckel et al., 2012; Wu et al., 2011). For this reason, testing the efficacy of the treatment in healthy elderly adults would represent the ideal proof of concept for this type of cognitive stimulation.

In addition, construct validity of the tasks included in the program was assessed with voxel-based correlational methodology (Tyler et al., 2005).

2. Material and methods

2.1. Participants

Adults older than 50 years without subjective cognitive complaints were enrolled from the population of the Venetian archipelago. A complete neurological screening led by a senior clinical neurologist was carried out on all candidates in order to rule out the presence of exclusion criteria, which were set as follows: cognitive impairment, significant pharmacological treatments with psychotropic medications, cholinesterase inhibitors, memantine, drugs for research purposes or with toxic effects to internal organs, a significant disease at clinical level, a previous history of transient ischemic attacks, a diagnosis of severe vascular pathology, a baseline structural MRI revealing a major diagnostic entity, presence/diagnosis of uncontrolled seizures, peptic ulcer, cardiovascular disease, sick sinus syndrome, neuropathy with conduction difficulties, significant disabilities, evidence of abnormal baseline levels of folates, vitamin B12 or thyroid stimulating hormone, significant depression/anxiety or other psychiatric conditions. A full neuropsychological-test battery was administered to determine absence of cognitive impairment. The scores obtained on the various cognitive tests were used for diagnostic purposes as well as baseline scores for the analysis of concurrent changes in cognitive abilities induced by cognitive stimulation.

All participants were invited to take part in the study and assigned to either the experimental or control groups. Forty-six individuals were enrolled, 27 of whom were allocated to the experimental condition. The anamnestic notes of all 19 participants assigned to the control condition were examined to ascertain that all carried out a stimulating lifestyle characterized by intense social contact. All these participants were, in fact, either still employed or engaged daily in organizational activities or voluntary work within the same setting where the experiment took place.

2.2. Network-based cognitive stimulation

A program of cognitive exercises was devised for the purpose of targeting aspects of connectivity which are down-regulated in healthy aging and, to a pathological level, in the early stages of AD. This resulted in the selection of specific cognitive domains, the coactivation of which would result into a strengthening of the patterns of functional connectivity of interest. Semantic processing, memory retrieval, logical reasoning, and executive processing were identified as computational domains adequate for the purpose and, at the same time, suitable for implementation into computerized exercises. Visuospatial and verbal materials were used to create computational activities which would rely on multiple cognitive abilities. As the main objective of each task was to tap distant hubs of the DMN concurrently, specific cognitive operations suitable for being combined in one task were selected. Although the design of a single stimulation task would have been sufficient to test the experimental hypothesis and, at the same time, would have allowed a "transparent" control of the mechanism by which engaging in the trials translates into regulation of functional connectivity, we decided to create multiple tasks. This choice was made both to confer a treatment-like aspect to the intervention, and to minimize the degree of potential monotony and boredom caused by the constant repetition of a single task for multiple sessions.

Identification of semantic characteristics and retrieval mechanisms were two cognitive processes persistently tapped by the tasks included in the program. By doing so, the intent was to induce simultaneous activity in widespread neocortical, and mediotemporal and limbic areas. This pattern of connectivity reflects part of the posterior component of the DMN. Further concurrent requests based on cognitive control were then added to foster functional connectivity between prefrontal and the aforementioned set of posterior limbic and neocortical regions, in order to regulate the DMN in its entirety. Flanker tasks were designed to exercise speed of processing and retrieval of proper names. In total, 20 sessions were created, each of which had to be completed within sixty to ninety minutes. The program was designed as intensive, as the complete package of sessions had to be completed within one month (ideally, 5 days a week for 4 weeks). In our study, participants enrolled in the experimental condition completed the program in an interval ranging between 20 and 42 days (mean: 25.05, standard deviation: 4.77)

As only a few studies have been carried out with a full awareness of the effects of an intensive cognitive stimulation program on neurocognitive variables (Whitlock et al., 2012), the creation of these activities was based on a model of AD-dependent decline in regional connectivity, with a concomitant involvement of distant areas, of crucial relevance in early-stage AD. Tasks were grouped into 5 clusters according to their main feature: semantic retrieval, logical reasoning, proper names retrieval, speed of processing, plus an extra "mind-twister" exercise administered as end of each daily session and consisting of a single trial. All tasks were administered through the E-Prime Software, Version 2.0 (Psychology Software Tools, Inc., Sharpsburg, PA). Accuracy and response times were recorded for all trials. The first session was slightly shorter than the others, and from the second session on, the material consisted of old and new trials mixed (1/3 old, and 2/3 new). The program was not tailored on individual performance but difficulty level changed progressively from session to session, and this was kept constant across all participants. The repeated trials were selected at random before the beginning of the training. The only task in which stimuli were tailored on individual performance was the proper-name retrieval task (see Section 2.2.4). Particular effort was put to set a gradually-increasing difficulty level along the twenty days of training, to ensure that the program was homogeneously challenging for its entire duration, as the participants proceeded throughout the training schedule. Verbal trials consisted of black-colored words and/or sentences on a white background. No participant complained about any of the physical features of the material (e.g. font size, font type, etc.). Similarly, image trials consisted of black-colored images on a white background. All original images were characterized by a realistic appearance and were not cartoonish or caricature-style. The Snodgrass-Vanderwart picture set (Snodgrass and Vanderwart, 1980) was used as the main source of stimuli, together with websites offering free educational material. Some images were specifically created for the purposes of this training. The participants were asked to respond to the trials by pressing a button on the keyboard. The keys necessary for the tasks were the spacebar and the 1, 2, 4, 5 key numbers located on the keypad on the right hand-side of a standard desktop keyboard. All stimuli appearing on the screen were accompanied by a number, and to respond to the trial the participants were asked to key in the number associated with the stimulus they wanted to choose. Instructions were always presented before the beginning of all tasks, for all sessions. Apart from the speed of processing tasks, the stimuli remained on screen until the participants gave their response. Although the training was centered on accuracy, rather than response time, the participants were asked to respond as soon as they had solved a trial.

2.2.1. Tasks based on semantic retrieval

The representation of semantic knowledge is associated with an extensive network of cortical areas within the parietal, temporal and frontal lobes which is visually similar to the DMN (Binder et al., 2009), and task-associated fMRI evidence indicates that semantic retrieval is involved in the DMN (Wirth et al., 2011). Engaging in tasks based on retrieval from the semantic system taps the activity of a set of areas which is very similar to the set of areas which activates when the system is at rest (Binder et al., 1999). This computational feature was particularly relevant in the creation of our training program because it helps elicit co-activation of the regions of the DMN both during as well as at the end of the tasks. For this reason almost all task modalities featured material with semantic content (e.g. words, sentences, images depicting objects or scenes). The tasks in this program of intensive cognitive stimulation included visual and verbal stimuli that could cover a big range of semantic content, with simultaneous computational requirements related to retrieval mechanisms, semantic ambiguity and interference, working memory, and inhibition. The neural substrate normally related to these extra components is located in key areas of the DMN, namely the mediotemporal formation, the anterior cingulate and the prefrontal cortex. The tasks were as follows:

2.2.1.1. Rule the odd one out 1. Four words were presented on screen. Three of these words belonged to the same semantic category, and one was unrelated to the other three. This alien word had to be identified and selected.

2.2.1.2. Rule the odd one out 2. Four images were presented on a computer screen. Similarly to the previous task, three of the images could be grouped in one category, while the fourth one did not fit with this category and had to be selected as the odd one out.

2.2.1.3. Dual category. Four words were presented on a computer screen as for the "rule the odd one out 1" task, but one of the words had a dual meaning. One of the two meanings was associated with two of the other words, whereas the second meaning was associated with the fourth stimulus, for example, RUBBER, RULER, PENCIL, and KING. RULER has two meanings; its first meaning is associated with RUBBER and PENCIL, and its second meaning is associated with KING. This semantic interference must be resolved by understanding which one is the meaning to select in order to obtain a category with 3 members and allow the completion of the trial by the final selection of the odd one out (KING, in this case).

2.2.1.4. Semantic inhibition. A sentence was presented on a computer screen and the participant had to read it carefully and keep it in mind. When they felt confident they could remember it, they had to press a key and 4 images were presented; the prior sentence was consistent with 3 of these images but made no sense with 1 of them, which had to be selected. In this task participants were not required to choose according to a "positive" feature (a match between cue and stimulus), but rather according to a "negative" feature (the only stimulus that did not match with the cue). As this was the last task of a sequence of activities in which "positive" features guide the response, it was necessary to inhibit the tendency to respond according to the detection of cue-stimulus matching.

2.2.2. Tasks based on logical reasoning

Evidence coming from fMRI research has revealed that the three sequential phases of deductive reasoning are associated with three different neural substrates: after the initial examination of the material, a phase based on evidence-gathering and integration follows, with prefrontal and occipito-temporal involvement, followed in turn by the validation phase, in which a prefrontal and parietal

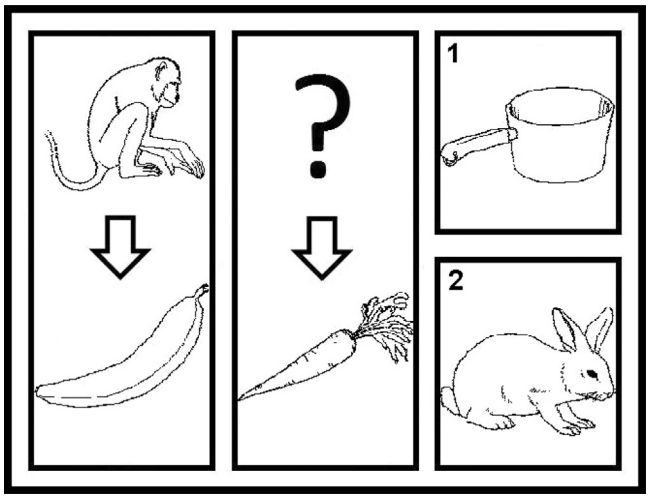

Fig. 1. Sample trial from the "sequence completion 2" task.
In order to solve this task, a series of cognitive steps have to be processed. First, a relation between the two images on the left ("monkey" and "banana") has to be determined. Once a candidate relation has been identified, it has to be transferred to the central compartment, where one of the two elements is missing ("question mark"). The sequence then has to be completed by inserting one of the two images presented on the right ("1: saucepan" and "2: rabbit") in the position signalled by the question mark. Both options (1 and 2) are semantically related with the item of the sequence ("carrot"), but only "rabbit" ensures that the same logical relation is maintained, as with "monkey" and "banana". This is a trial in which the solution is simple, as it has a large degree of imageability. More difficult trials were characterized by abstract or indirect inter-image relations (e.g. "bear" and "bee" on the left, "cat" in the upper central position, "1: milk" and "2: cow" as the alternative answers on the right).
The "sequence completion 1" task consisted of the same procedure applied to verbal material (i.e. words). Since verbal material is independent from its visual imageability, terms indicating abstract concepts were often used.

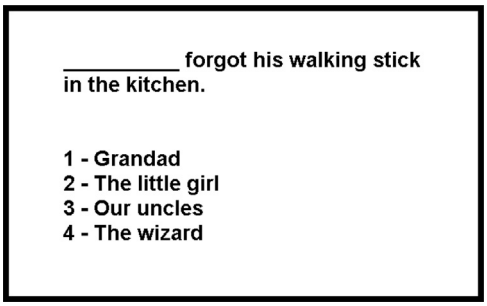

Fig. 2. Sample trial from the "sentence completion" task.
This task requests the participant to choose the best of the four alternatives presented in the lower part of the screen, which can complete the upper sentence. Very often a process of elimination has to be put into practice to rule out the options which are not viable. For this specific trial the selection of option number 3 would read wrong, as it would generate a morphological mismatch. Grammar-wise, the remaining options are all possible, but the semantics associated with the elements suggests that option number 4 is not likely to be the answer, as "wizard" and "kitchen" typically do not share the same conceptual scenario (as opposed to "wizard" and "castle", for instance). At this point, both remaining options (1 and 2) can work out as correct answer, but option number 1 is the only one requiring no further implications (specifying whom "his" refers to, if option number 2 were to be chosen), and is, therefore, the correct option.

circuit is recruited (Fangmeier et al., 2006). Based on this piece of evidence, we created tasks of logical deductive reasoning in which strong semantic processing was required to select the correct answer.

2.2.2.1. Sequence completion 1. Two words were presented on the left side of a computer screen, connected by an arrow. A relation existed between these two words. The same relation was repeated for other two words in the middle of the screen, similarly connected by an arrow; however, one of these was missing (and substituted by a question mark). Two other words were located on the right side of the computer screen and one of them represented the correct answer to complete the sequence. Both choices were semantically related with the available word, but only one of them would ensure that the logical sequence is respected following the same relation between the two guide-words presented on the left of the screen.

2.2.2.2. Sequence completion 2. This task was as the "sequence completion 1" task, but this time no words were presented and the deductive reasoning had to be performed based on image stimuli only (e.g. Fig. 1).

2.2.2.3. Sentence completion. A sentence was presented in the top half of the screen, with one element missing (the subject, the verb, or a complement). Four possible choices were available in the bottom half of the screen and only one represented the correct answer. The response had to be found by a process of elimination in which one or two options could be logically ruled out, and very often a semantic feature was crucial to make the final choice (e.g. Fig. 2).

2.2.2.4. Scene completion. A complex scene was presented in the middle of the screen, in which an element had been removed (the main element, the background or a detail). Four smaller images were presented at the four corners of the screen and the participant had to select the image that best completed the scene. Similarly to the "sentence completion" task, the final choice had to be made based on logical and semantic elements.

2.2.3. Tasks based on response time

Response time is considered a basic executive component contributing significantly to efficient processing. Evidence has shown how faster participants performing a modified version of the Digit Symbol Modalities Task in a go-no-go form have a larger activation within parietal areas and reduced activation within certain prefrontal regions than slower adults (Rypma et al., 2006), in line with the idea that faster cognitive performance is mirrored by a more efficient neural computation, interestingly described as a partial anterior down-regulation and posterior up-regulation. We created 4 simple tasks in which we specifically asked the participants to press a key as rapidly as possible. Stimulus onset asynchrony was variable to avoid facilitation of response.

2.2.3.1. Respond to A. A fixation cross was presented, followed by a capital A, appearing in the center of the screen. The participant had to press a button as quickly as possible when they saw the stimulus.

2.2.3.2. Respond to the square. This was similar to the "respond to A" task, but the stimulus to respond to was a blue square.

2.2.3.3. Respond to A and B. After the fixation cross a capital A or B could appear in the center of the screen. The participant had to press one of two different keys as quickly as possible depending on which stimulus was presented.

2.2.3.4. Respond to red and blue squares. This task was similar to the previous one, but the differential response was driven by the color of the square.

2.2.4. Proper name retrieval

Recalling the name and/or surname of a well-known person is a difficulty that older people very often complain about, and it has been objectively described in mild cognitive impairment (MCI) together with an impairment of other forms of proper name retrieval (Ahmed et al., 2008). A factor analysis revealed that

phonological access problems seem to underlie the concurrent tip-of-the-tongue phenomenon with proper names in MCI individuals (Juncos-Rabadán et al., 2011). Proper names for people or for topographical/geographical places are processed by a network of areas that has not been yet fully understood (Yasuda et al., 2000). We chose to include this task as a "symptomatic" activity for participants, as it is a very common complaint manifested during neurological examination. A brief written description (1 or 2 sentences) of a very famous person/place was presented on the screen. The participant had to read it and communicate the name corresponding to the description to the tester. If the participant could not retrieve the name, additional details about the person/place were given. If the participant still could not come up with the answer, this was provided by the tester, and the same trial would be asked on the following day in addition to the new trials. If the participant could still not recall the answer on the following day, the first letter of the name or first letter of name and surname were given as a cue. If the response was not given, additional letters were given, up to a total of four cues. If the participant still could not give the answer after 4 cumulative cues, this was provided by the tester. Whenever the response could not be given without the help of a cue, the trial was re-asked in the next session. Since this approach is errorless, no information about accuracy or response time was registered.

2.2.5. Mind-twister filler

A single-trial task was created, based on lexical-semantic processing. This task was not part of the program, but served as a filler task in case the tester needed to focus on a problematic trial with one participant and could not dedicate much time to other participants. It also served as a final task for participants that joined the experiment together (e.g. husband and wife) but one of them finished earlier than the others (see Section 2.3 for procedural details on multiple-participant sessions). It was preferentially left at the end of the session, as it was very stimulating, challenging and was well received by participants, who left the lab and the hospital in a positive mood. Sometimes the response was given immediately, sometimes more time was needed. Three words were presented on a computer screen, completely unrelated with each other. The task was to find a fourth word that was verbally related to each of the stimuli in specific expressions and ways of saying, in which the global meaning was beyond the simple apposition of the terms. For instance a potential trial in English could be: TWISTER, CHEEK, and MOTHER. The response is TONGUE, as TONGUE-TWISTER, TONGUE-IN-CHEEK and MOTHER TONGUE represent three semantic constructs independent from the literal combination of cue and target.

2.3. Procedure

The stimulation laboratory consisted of four separate workspaces equipped with desk and computer, placed at the four corners of the room and facing against the wall. Simultaneous treatment for multiple participants was possible. The tester was present in the room for the full time of the stimulation and no other people had access to the laboratory during this time. Participants were asked to carry out their individual work in silence and were allowed to ask for assistance in case of difficulty. The tester was in charge of the start-up of all tasks for all participants, who were instructed to wait for the tester at the end of their performance on a task. The order of the tasks was randomly chosen by the tester, to avoid the scenario of multiple participants finishing a task at the same time and waiting for too long before starting a new one, and to save sufficient time to allow all participants to perform the "proper name retrieval" task with discretion (and in a low voice) together with the tester. Participants were also allowed to take advantage of the numerous pauses between and within tasks. The tester supervised the training and was at hand if help were needed. In such cases no specific help with the trial was given, but rather a refresh of task instructions with emphasis on the problematic trial was provided. As for the time of training, it was scheduled on a day-by-day basis by participant and tester together, and to ensure compliance participants were allowed to attend the lab at a flexible (morning to evening), and variable (e.g. Monday at 8am and Tuesday at 2pm) schedule, even if another participant had already started their session. Out-of-phase sessions were possible, with simultaneous training of participants who were at different stages (e.g. participant 1 performing session 4/20 together with participant 2 performing session 7/20). This flexibile regime was adopted to maximize compliance with the training. Timing of individual sessions was scheduled taking into account individuals' preference and never imposed by the examinaner.

This study received ethical approval by the IRCCS Fondazione Ospedale San Camillo (Venice, Italy) institutional ethics committee (reference number CE: Protocollo 11.07). Written informed consent for participation was obtained from all recruited individuals.

2.4. Battery of cognitive tests

A comprehensive battery assessing various aspects of cognition was put together with particular focus on those aspects mostly targeted by normal and pathological aging. The Digit Span Forward (Orsini et al., 1987) and Backwards served as measures of verbal short term and working memory; the spatial span was measured with the Corsi Test (Orsini et al., 1987). The Rey-Osterrieth complex figure (Caffarra et al., 2002a; Osterrieth, 1944; Rey, 1941) was used as a measure of visuoconstructive skills (copy) and visual long-term memory (10-min delayed recall). Verbal memory was assessed with the Prose Memory Test (Novelli et al., 1986a) and the Paired Associates Test (Novelli et al., 1986a). Lexical and semantic skills were tested with the Letter Fluency Test (Novelli et al., 1986b) and the Category Fluency Test (Novelli et al., 1986b). The Digit Cancellation Test (Spinnler and Tognoni 1987) was used as a measure of visual search and speed of processing; a component of executive functioning was assessed with the short version of the Stroop Test (Caffarra et al., 2002b; Stroop, 1935; Venneri et al., 1993). The Token Test (Spinnler and Tognoni 1987) was chosen as a measure of comprehension and receptive language; the Similarities Test from the Wechsler Adult Intelligence Scale-Revised battery (Wechsler, 1981) and the Raven Progressive Matrices (Raven, 1947; Basso et al., 1987) were respectively chosen as verbal and non-verbal measures of abstract reasoning. Raw scores on tests were corrected for age and level of education (some also for gender) for clinical purposes, using various sources of normative data except for the Digit Span Backwards for which no normative data exist for the relevant population. Corrected scores were finally converted into equivalent scores (0–4), which were used for diagnostic purposes.

2.5. MRI acquisition and preprocessing

Echo planar T2* weighted MRI sequences and T1 weighted anatomical images were acquired on a 1.5 T Philips Achieva system as part of a comprehensive scanning protocol. This also included T2 weighted and FLAIR scans to allow the evaluation of vascular load and the detection of other possible clinical abnormalities, as part of the evaluation of exclusion criteria.

The acquisition parameters of T2* images were set as follows: TR = 2 s, echo delay time = 50 ms, flip angle 90°, voxel dimensions $3.28 \times 3.28 \times 6.00$ mm, field of view 230 mm. Two 120-volume runs of 20 contiguous axial slices acquired in ascending order were obtained for each participant. Twenty seconds of preliminary dummy scans allowed the scanner to reach equilibrium. Three-dimensional T1 weighted structural scans were acquired

with a Turbo Field Echo Sequence, and acquisition parameters were set as follows: voxel dimension: 1.1 × 1.1 × 0.6 mm; field of view: 250 mm; matrix size 256 × 256 × 124; TR: 7.4 ms, TE: 3.4 ms; flip angle: 8°. Similarly to the procedure described by Han et al. (2012), no specific instructions were given to participants during the MRI sessions, except for the recommendation to remain still for the whole duration of the scans.

T2* and T1 sequences were preprocessed and analyzed using the Statistical Parametric Mapping (SPM) 8 software (Wellcome Trust Centre for Neuroimaging, London, UK) implemented in Matlab 7. All echo planar scans were initially slice-timed, and each of the two sessions of volumes was realigned independently. Realignment procedures were carried out using the 4th Degree B-Spline Interpolation option. Mean volumes were created as reference, and parameters of linear and rotational head motion were estimated. These were visually inspected to identify head movements which could have impacted on subsequent analyses. During this visual inspection peaks of linear and rotational movement exceeding 1.5 mm and 3°, respectively, were identified as problematic. After realignment, images were then normalized using the first realigned volume of the first session as source image to match the default echo-planar template available in SPM 8, and voxel size was isotropied at 2.0 × 2.0 × 2.0 mm. A band-pass filter was applied to normalized sequences to remove frequencies not believed to result from the expression of neural activity. This was carried out using the REST toolbox (www.restfmri.net) (Song et al., 2011). Similar to the majority of studies on BOLD signal, a low-pass filter was set at 0.1 Hz to eliminate frequencies generated by physiological mechanisms (Fox and Raichle, 2007). A high-pass filter was also set at 0.008 Hz to remove low-frequency drift, as carried out in other studies (e.g. Harrison et al., 2008). Finally, band-pass filtered volumes were smoothed with a 6 mm^3 full-width at half maximum gaussian kernel to account for any possible inter-subject differences remaining after normalization, and to improve signal-to-noise ratio.

Voxel-Based Morphometry (VBM) preprocessing was carried out on anatomical scans. Manual reorientation of the images was initially performed to facilitate a successful overlap with the SPM 8 template of Caucasian brains. Reoriented scans were then segmented to allocate each voxel to one of the three maps of tissue category (gray matter (GM), white matter (WM), and cerebrospinal fluid (CSF)), according to a probabilistic value. Subjective GM and WM maps were then transformed to a stereotactic space to match the template and achieve normalization. A visual examination of the output was then carried out to check the quality of the segmented images, which were finally smoothed with a 8 mm^3 full-width at half maximum gaussian kernel. Unprocessed native-space GM, WM and CSF maps served for the purpose of calculating total intracranial volumes (TIV; $TIV = Vol_{GM} + Vol_{WM} + Vol_{CSF}$), and tissue-category ratios ($Ratio_{GM} = Vol_{GM}/TIV$; $Ratio_{WM} = Vol_{WM}/TIV$; $Ratio_{GM+WM} = (Vol_{GM} + Vol_{WM})/TIV$).

The visual inspection of T1 scans after segmentation revealed no abnormalities in the segmentation procedure. Two T2* runs were indicated as problematic by the examination of motion parameters. Fifteen and 40 volumes were removed from these two runs, respectively, and their entire preprocessing procedure was re-run. These two removals did not generate temporal discontinuity in the two datasets.

2.6. Analytical procedures

2.6.1. Creation of a DMN template

After preprocessing, group independent component analysis (ICA) was performed on all baseline functional scans. This was completed solely to identify the DMN template of the recruited sample to be used for further analyses. The GIFT toolbox (GIFT v1.3i; mialab.mrn.org/software/gift) was used for this purpose (Calhoun et al., 2001). Briefly, an initial principal component analysis was carried out to reduce the number of sources of variability, and the Infomax algorithm was then chosen to perform the ICA. Finally the GICA method was selected for back reconstruction, in which participant-specific spatial maps and time-courses were estimated. Similar to other published studies (i.e. Rosazza et al., 2012), the number of components to be computed was set at 20. Only one single output component was reputed to show the spatial characteristics of the DMN. Since the rater-dependent selection of the DMN from the ICA output shows almost perfect inter-rater reliability (Franco et al., 2009), the *z*-score map of the appropriate component was visually identified and extracted from all individual sets of components. A one-sample *t* test was then carried out using SPM 8 on the whole set of baseline DMN maps ($p < 0.001$ uncorrected, cluster extent: 100 contiguous voxels), and a mask was then created based on this output. This mask included all DMN areas described in the Introduction session, and, similarly to the procedure described in other studies (e.g. Bozzali et al., 2015), served as spatial constraint for all subsequent statistical inferences (Fig. 3).

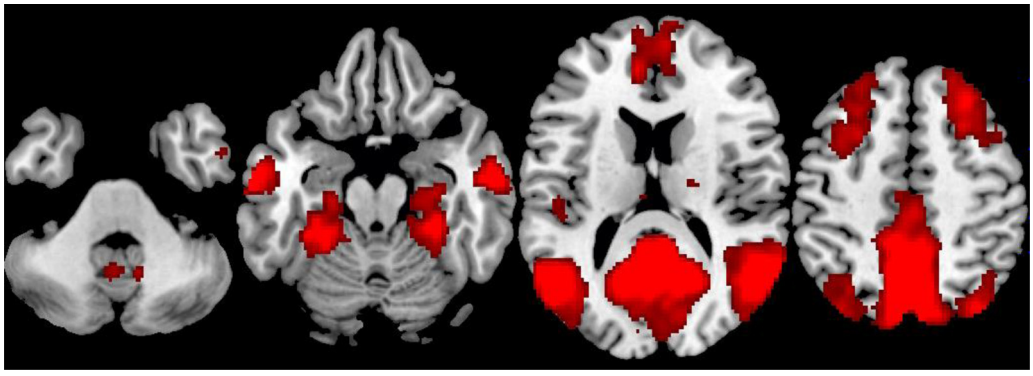

Fig. 3. DMN mask used in the analyses of the study. (For interpretation of the references to color in this figure, the reader is referred to the web version of this article)
A group-level independent component analysis was run on the entire set of baseline fMRI scans (experimental and control group together), and the component showing the spatial features typical of the DMN was extracted for each participant. A one-sample *t* test was then run on the entire set of maps ($p < 0.001$, cluster extent ≥ 100 contiguous voxels). The figure shows the resulting map, which was subsequently binarized for masking purposes. The group-level DMN estimated with this procedure was highly symmetric, and included a large postero-medial cluster covering the entire posterior-cingulate and precuneal regions, a large portion of the inferior parietal lobe, including the angular and supramarginal gyri, the lateral temporal cortex (mainly extending to the middle temporal gyrus), the hippocampal and parahippocampal regions, the medial prefrontal cortex, the thalamus, a small portion of the cerebellum centered on lobule IX, and part of the dorsal prefrontal cortex.
MNI coordinates of the slices are as follows: $z = -38, -20, 15, 50$.

2.6.2. Association between task performance and brain structure

Construct validity of each single task modality was measured in the group of adults participating in the experimental condition of the study, and was assessed using a voxel-based correlation methodology, following the procedure described in the study by Tyler et al. (2005). Linear multiple regression models were run, including baseline maps of smoothed GM as dependent variable, and task performance as main regressor. Average scores were calculated to characterize the performance on every single task modality over the first three sessions of the stimulation program. Since error rates showed insufficient statistical variability (mainly because of a trend toward a ceiling effect), response times were used. In addition, response times were preferred over accuracy rates because they represented a more genuine proxy of the computational process of induced co-activation, which was expected to occur regardless of whether the correct response was subsequently given. Positive associations were calculated, in order to identify the sets of areas where more GM was associated (and, possibly, "necessary", if causality were to be speculated) with longer response times. For tasks based on response time, a difference score was computed to negate the influence of the perceptual or motor features of the task, and to identify an estimate of pure decisional speed. A negative association was calculated between this score and GM maps to identify the GM configuration associated with quicker decisional speed. Age, educational levels and $Ratio_{GM}$ were included as nuisance regressors in all models.

2.6.3. Computation of individual DMN maps

A seed-based approach was used to estimate DMN maps, as previously carried out elsewhere (Machulda et al., 2011). Two spherical (radius: 5 mm) Regions of Interest (ROI) were created using the MARSeille Boîte À Région d'Intérêt (MarsBaR) toolbox (marsbar.sourceforge.net) (Brett et al., 2002). These were drawn in the retrosplenial portion of the posterior cingulate, one in each hemisphere (MNI coordinates: $x = \pm 7$, $y = -51$, $z = +14$). These coordinates were chosen based on structural atlases, and attention was paid not to include any voxel of the intra-hemispheric sulcus, in order to avoid miscalculations of average ROI signal due to absence of cortical tissue and presence of CSF. The mean ROI signal was extracted from the smoothed scans keeping the two runs separate. Two other ROIs covered instead the entire map of WM and CSF, respectively, and were created by segmenting the 3D T1 template contained in SPM 8. First-level analyses aimed at creating individual maps of functional connectivity of the two posterior-cingulate seeds. The average time-courses computed within the WM and CSF map were regressed out, as well as the motion parameters previously estimated during realignment. Although the structural integrity of the cortex may influence functional connectivity (Damoiseaux et al., 2012), no correction for GM volumes was applied. This choice was made based on the longitudinal nature of the design, which should be sufficient to control for the influence of individual differences in cortical integrity.

2.6.4. Statistical analysis

A between-subject factor (group) and a within-subject factor (time-point) were inputted in full-factorial second-level models, as well as in models testing the impact of treatment on volumetric maps. The interaction effect was assessed to determine the differential increase in volumes and connectivity obtained in the experimental condition. The "inverse interaction" contrast (determining the exclusive increases in volumes and connectivity seen in the control condition) was also inferred. For the analysis of GM and WM changes, TIV and $Ratio_{GM}$ (or $Ratio_{WM}$, depending on the analysis) were used as correction factors. Whenever an interaction reported significant findings, additional paired *t* tests were run to characterize neural increases and decreases within each of the two groups.

For all analyses, a cluster extent of at least 15 contiguous voxels was selected, and the *p* value was set at 0.005, uncorrected. This statistical threshold was previously judged as the best compromise in test-retest designs in samples of MCI patients (Fouquet et al., 2009). All peak coordinates were reported as significant only if they survived a $p < 0.05$ Family-Wise Error corrected *D* statistic at a peak level.

Peak coordinates were transformed in Talairach stereotaxic space using the Matlab function mni2tal (http://imaging.mrc-cbu.cam.ac.uk/downloads/MNI2tal/mni2tal.m) and results were interpreted using the Talairach Daemon client (www.talairach.org/client.htm). Peak values were processed using the "Nearest Gray Matter" database search option (aside from the interpretation of WM changes).

Global changes in Vol_{GM}, Vol_{WM}, $Ratio_{GM}$, $Ratio_{WM}$ and $Ratio_{GM+WM}$ were analyzed with IBM Statistical Package for the Social Sciences (SPSS) 21 software. Similar to the neuroimaging procedures, mixed ANOVAs were run and interpreted.

Changes in raw neuropsychological scores were analyzed with SPSS 21. Again, comparably to neuroimaging analyses, mixed ANOVAs were run to test the group-by-time-point interaction for each of the cognitive tests. Age and educational levels were added as covariates. The significant threshold was divided by the number of statistical comparisons ($n = 16$) (Bonferroni correction), in order to rule out Type 1 error inflation ($p < 0.0031$). Since these analyses were exploratory in nature, assumptions for parametric statistics were not checked.

2.7. Exclusions from the study

Four individuals participating in the experimental condition of the study did not undergo MRI scanning, either because of medical contraindication or claustrophobic crisis. For this reason they were excluded from the study, as well as a fifth participant of the experimental group, who showed a vast traumatic lesion suffered during early development. Finally, one participant withdrew and did not complete the training program, reducing thus the size of the experimental group to 20 individuals. Since, however, this sixth participant had completed more than three treatment sessions, they were suitable for inclusion in the analyses of task construct validity.

A seventh participant, enrolled in the control group, was offered the entire treatment at the end of all retest procedures. By doing so, their retest scan was used in the analysis of construct validity.

The baseline demographic characteristics of the remaining 40 participants included in the analyses of treatment effects are illustrated in Table 1. No difference was found for these variables.

Table 1
Demographic characteristics of the recruited participants.

	Complete sample	Experimental group	Control group	$p_{\text{values group difference}}$
Age	65.90 (8.53)	66.81 (7.65)	64.74 (9.29)	0.444
Education	10.95 (4.50)	10.52 (4.45)	11.47 (4.82)	0.521
Gender (F/M)	26/14	14/7	12/7	0.816

Group-differences were tested with independent-sample *t* tests (age and education) or Pearson $\chi 2$ test (gender).

Furthermore, the two groups showed comparable levels of cognitive performance in the baseline neuropsychological assessment. To determine this, between-sample ANOVAs (correcting for age and educational levels) were carried out, and no difference emerged (all p values > 0.0031, see Table 2).

3. Results

3.1. Association between task performance and brain structure

The pattern of association between GM maps and task performance is illustrated in Table 3. Overall, the set of DMN areas showing significance were mainly located in the temporal cortex, in the precuneus and other parietal areas and in mediotemporal clusters. An association with prefrontal GM was only found for tasks specifically based on logical reasoning or response time.

3.2. Treatment effect on functional connectivity

The full-factorial design revealed a significant effect of the interaction on functional connectivity of both seeds. The entire set of areas is listed in Table 4 and is illustrated in Fig. 4.

The interaction contrast revealed increased connectivity between the left seed and the right precuneus, the cuneus bilaterally, the right inferior parietal lobule and the right middle frontal gyrus. A single decrease was instead found in the ventral portion of the left parahippocampal gyrus (not included in Fig. 4). Overall, the analysis of the right seed revealed a comparable pattern of findings. The interaction model indicated increased functional connectivity between the right posterior cingulate and the left precuneus, cuneus, superior parietal, and temporal cortices. Additionally there also was increased connectivity with the left parahippocampal gyrus.

This configuration was consistent with paired t tests carried out on each of the two groups, separately. The entire set of findings emerging from this set of additional analyses is reported in Table 5.

Limited increase in seed-based connectivity was found in those who did not receive treatment. This latter group showed a pattern of decreased connectivity, extending to the right parietal cortex and precuneus, and to other bilateral clusters located in the temporal, parietal, and occipital cortices. Complementarily, connectivity of the posterior cingulate was up-regulated by the training. This was evident mainly in the precuneus, bilaterally, and extended to right frontal areas, the right parietal cortex, and left temporal and occipital clusters. Only a few decrements in connectivity were reported in the group of treated adults, and, these did not affect any key areas of the DMN.

3.3. Treatment effect on volumetric measures

The numerical analyses revealed no change in global GM and WM volumes or ratios (see Table 6). A significant group-by-time-point interaction was instead reported by the VBM analysis of GM volume. This extended to the left anterior cerebellum and the left fusiform gyrus (see Table 7 and Fig. 5). Additional t tests (reported in Table 8) indicated that the group who had received treatment had increased GM volumes in these structures, while no change was observed in the control group. The t tests indicated also a significant mediotemporal and limbic volumetric decrease in the control group. No change in WM volumes was triggered by the program.

3.4. Treatment effect on cognitive abilities

The impact of the stimulation program on the performance over the battery of neuropsychological tests is reported in Table 2.

Table 2
Cognitive performance as measured by the battery of neuropsychological tests.

Test	Cut-off	Experimental condition			Participants scoring below cut-off	Control condition			Participants scoring below cut-off	p_{ANOVA} baseline group difference	p_{ANOVA} treatment effect
		Baseline	Retest	n		Baseline	Retest	n			
Raven's progr. matrices	≤18.96	30.76 (4.56)	32.48 (2.87)	21	0	31.47 (4.23)	30.58 (5.13)	19	0	0.865	0.017
Letter fluency	≤16	32.62 (13.89)	40.14 (12.54)	21	2	44.05 (11.69)	43.42 (10.88)	19	0	0.015	0.004
Category fluency	≤24	42.90 (11.63)	46.52 (11.64)	21	1	44.32 (8.11)	45.16 (6.90)	19	0	0.948	0.384
Digit cancellation	≤30	54.67 (4.61)	54.76 (3.96)	21	0	54.89 (4.12)	56.58 (3.29)	19	0	0.874	0.228
WAIS similarities	N.A.	20.67 (4.32)	22.00 (3.53)	21	N.A.	21.37 (5.29)	22.26 (4.47)	19	N.A.	0.830	0.683
Token test	≤26.25	34.92 (1.17)	34.92 (1.15)	20	0	35.08 (1.38)	35.18 (1.17)	19	0	0.925	0.740
Rey figure—copy	≤28.87	32.90 (3.33)	34.00 (3.74)	21	2	32.58 (2.97)	32.87 (2.91)	19	1	0.645	0.516
Rey figure—recall	≤9.46	17.02 (6.22)	19.90 (6.97)	21	1	15.63 (6.36)	18.18 (7.07)	19	2	0.284	0.766
Stroop test—time	≥36.92	18.71 (7.15)	18.71 (8.25)	21	0	22.99 (8.34)	20.76 (7.88)	19	0	0.016	0.165
Stroop test—errors	≥4.24	0.60 (1.30)	0.29 (0.64)	21	0	0.53 (1.31)	0.11 (0.32)	19	0	0.893	0.573
Digit span forward	≤3.5	6.00 (0.71)	6.00 (0.89)	21	0	5.89 (0.81)	6.21 (0.86)	19	0	0.549	0.220
Digit span backwards	N.A.	4.19 (1.03)	4.52 (1.03)	21	N.A.	4.47 (0.77)	4.16 (0.90)	19	N.A.	0.504	0.043
Corsi test	≤3.25	4.86 (0.91)	4.81 (0.75)	21	0	4.68 (0.58)	5.05 (0.97)	19	0	0.284	0.096
Prose memory test—immediate	N.A.	8.81 (3.08)	11.86 (4.75)	21	N.A.	9.79 (2.82)	11.32 (3.30)	19	N.A.	0.404	0.252
Prose memory test—delayed	N.A.	12.10 (4.45)	14.67 (4.84)	21	N.A.	13.21 (3.90)	15.58 (3.73)	19	N.A.	0.594	0.764
Prose memory test—total score	≤15.75	20.90 (6.85)	26.52 (9.13)	21	5	23.00 (6.13)	26.89 (6.10)	19	2	0.316	0.340
Paired associates	≤6	13.17 (3.10)	14.02 (4.85)	21	0	12.32 (3.06)	13.00 (3.96)	19	0	0.304	0.756

Means and standard deviations are indicated. The baseline Token test score was not measured for one of the participants in the experimental condition. Cut-offs reported in the table reflect age-, education- and gender-corrected values separating normal from abnormal cognitive performance, as indicated by normative data previously published (see references included in Section 2.4).
Significant threshold: $p < 0.0031$.

Table 3
Association between task performance and regional GM volumes.

Brain region	Side	BA	Cluster size (voxels)	*Z* score at local maximum	D_{FWE} at peak level	Talairach coordinates		
						x	*y*	*z*
Semantic retrieval—rule the odd one out 1								
Precuneus	L	7	36	3.68	0.004	−8	−71	51
Middle temporal gyrus	R	21	21	3.54	0.006	57	−18	−11
Angular gyrus	L	39	19	3.41	0.009	−50	−66	35
Inferior parietal lobule	L	39	15	2.98	0.029	−48	−64	44
Middle cingulate gyrus	R	31	45	3.31	0.012	4	−27	36
Middle cingulate gyrus	L	31	24	3.08	0.023	−6	−31	33
Angular gyrus	R	39	15	3.27	0.014	57	−61	33
Middle temporal gyrus	L	37	10	3.16	0.018	−53	−62	7
Middle temporal gyrus	L	19	16	3.11	0.021	−48	−63	12
Semantic retrieval—rule the odd one out 2								
Middle temporal gyrus	L	37	18	3.98	0.002	−53	−62	7
Angular gyrus	R	39	19	3.85	0.002	57	−61	33
Precuneus	L	7	45	3.84	0.003	−8	−69	51
Middle cingulate gyrus	R	31	54	3.62	0.005	4	−27	36
Middle cingulate gyrus	L	31	53	3.56	0.006	−4	−31	35
Angular gyrus	L	39	14	3.52	0.007	−48	−66	35
Inferior parietal lobule	L	39	22	3.25	0.015	−46	−66	44
Precuneus	L	19	11	2.81	0.043	−40	−72	44
Middle temporal gyrus	R	21	20	3.29	0.013	59	−46	10
Superior occipital gyrus	L	19	14	3.02	0.026	−40	−84	26
Hippocampus	R		6	3.19	0.017	30	−31	−6
Middle temporal gyrus	L	21	14	3.13	0.020	−59	−18	−14
Inferior temporal gyrus	L	21	9	2.93	0.033	−59	−5	−13
Semantic retrieval—dual category								
Posterior cingulate	L	30	45	4.01	0.001	−8	−50	19
Middle cingulate gyrus	L	31	64	3.83	0.003	−4	−33	35
Middle cingulate gyrus	R	31	59	3.69	0.004	6	−41	28
Middle temporal gyrus	L	37	22	3.79	0.003	−53	−62	7
Middle temporal gyrus	L	21	21	3.79	0.003	−59	−54	6
Middle temporal gyrus	L	39	32	3.39	0.010	−42	−71	26
Parahippocampal gyrus	R	36	35	3.74	0.004	20	−37	−7
Precuneus	L	19	24	3.69	0.004	−38	−80	39
Angular gyrus	L	39	16	3.59	0.006	−48	−66	35
Precuneus	L	7	34	3.58	0.006	−8	−71	51
Parahippocampal gyrus	L	35	14	3.50	0.007	−26	−20	−17
Paracentral lobule	L	5	16	3.46	0.008	−16	−36	48
Middle temporal gyrus	R	21	35	3.37	0.011	59	−46	10
Thalamus	R		23	3.24	0.015	6	−12	−1
Thalamus—medial dorsal nucl.	R		46	3.07	0.023	6	−19	5
Middle temporal gyrus	R	37	7	2.80	0.044	61	−45	−6
Thalamus—pulvinar	L		38	3.02	0.027	−12	−27	3
Thalamus—medial dorsal nucl.	L		59	2.97	0.030	−6	−19	5
Thalamus	L		6	2.77	0.048	−4	−10	0
Hippocampus	R		5	2.92	0.034	30	−31	−5
Supramarginal gyrus	L	40	4	3.00	0.028	−50	−49	25
Semantic retrieval—semantic inhibition								
Superior temporal gyrus	L	22	32	4.03	0.001	−51	−50	17
Middle temporal gyrus	L	19	53	3.76	0.003	−48	−59	16
Middle occipital gyrus	L	19	24	3.39	0.010	−34	−67	16
Middle cingulate gyrus	L	31	67	3.87	0.002	−8	−39	35
Middle cingulate gyrus	R	31	39	3.55	0.006	6	−27	38
Paracentral lobule	L	5	13	3.78	0.003	−18	−38	48
Middle temporal gyrus	L	21	25	3.72	0.004	−50	1	−24
Middle temporal gyrus	R	21	31	3.55	0.007	63	−18	−11
Inferior temporal gyrus	R	20	21	2.98	0.030	59	−13	−21
Lingual gyrus	R	30	30	3.54	0.007	20	−41	−1
Parahippocampal gyrus	R	36	38	3.43	0.009	28	−32	−10
Parahippocampal gyrus	R	35	33	3.43	0.009	22	−35	−7
Parahippocampal gyrus	L	35	24	3.53	0.007	−24	−22	−19
Parahippocampal gyrus	L	36	31	3.47	0.008	−34	−34	−12
Parahippocampal gyrus	L	27	18	3.38	0.011	−22	−35	−2
Middle temporal gyrus	R	39	47	3.50	0.008	42	−63	23
Cuneus	R	23	11	3.42	0.009	10	−71	9
Cuneus	R	17	14	3.25	0.015	18	−73	9
Cuneus	R	30	16	3.06	0.024	24	−69	13
Superior temporal gyrus	R	22	16	3.39	0.010	59	−48	15
Posterior cingulate	L	31	20	3.09	0.023	−6	−55	25

Table 3 (*Continued*)

Brain region	Side	BA	Cluster size (voxels)	*Z* score at local maximum	D_{FWE} at peak level	Talairach coordinates		
						x	*y*	*z*
Logical reasoning—sequence completion 1								
No results								
Logical reasoning—sequence completion 2								
Middle frontal gyrus	R	8	28	4.23	0.001	32	17	36
Superior frontal gyrus	L	8	20	4.19	0.001	−16	39	46
Superior occipital gyrus	L	19	23	3.74	0.003	−40	−80	33
Precuneus	R	7	27	3.55	0.006	16	−60	42
Superior parietal lobule	L	7	16	3.32	0.012	−32	−56	51
Superior frontal gyrus	R	8	16	3.10	0.022	28	26	48
Logical reasoning—sentence completion								
No results								
Logical reasoning—scene completion								
Middle cingulate gyrus	R	31	19	3.85	0.002	14	−41	43
Decisional speed								
Superior temporal gyrus	R	39	41	4.17	0.001	55	−61	18
Precuneus	L	7	24	3.68	0.004	−4	−50	56
Cuneus	L	23	34	3.44	0.009	−10	−75	11
Cuneus	L	17	63	3.31	0.012	−2	−79	11
Cuneus	R	18	20	2.89	0.036	4	−85	12
Medial frontal gyrus	L	9	29	3.42	0.009	−4	47	16
Cuneus	R	19	42	3.31	0.013	2	−76	33
Precuneus	R	31	12	3.01	0.027	8	−65	27
Supramarginal gyrus	R	40	15	3.29	0.013	61	−51	30
Middle frontal gyrus	R	8	26	3.28	0.013	28	29	43
Cuneus	L	19	14	3.21	0.016	−26	−84	28
Precuneus	R	19	13	3.10	0.021	32	−72	31

The inferential statistics was corrected for Family-Wise Error but, given the exploratory nature of these analyses, no correction for multiple models was applied.
BA: Brodmann area, L: left, R: right.

Table 4
Analysis of seed-based connectivity of the posterior cingulate as measured by group-by-time-point interactions.

Brain region	Side	BA	Cluster size (voxels)	*Z* score at local maximum	D_{FWE} at peak level	Talairach coordinates		
						x	*y*	*z*
Left seed—interaction								
Precuneus	R	7	15	3.52	0.006	6	−64	49
Cuneus	R	18	34	3.50	0.006	18	−73	20
Posterior cingulate	R	30	17	2.87	0.036	24	−69	9
Inferior parietal lobule	R	39	22	3.42	0.008	48	−66	42
Middle frontal gyrus	R	8	17	3.40	0.008	34	16	42
Inferior temporal gyrus	R	21	15	3.24	0.013	59	−8	−13
Precuneus	R	19	36	3.21	0.015	38	−78	37
Cuneus	L	18	28	3.11	0.019	−2	−79	19
Cuneus	L	19	19	3.10	0.020	−26	−86	32
Angular gyrus	L	39	21	3.01	0.025	−44	−72	31
Left seed—inverse interaction								
Parahippocampal gyrus	L	35	23	3.21	0.015	−14	−29	−7
Right seed—interaction								
Parahippocampal gyrus	L	35	13	3.95	0.001	−22	−24	−21
Superior parietal lobule	L	7	39	3.57	0.005	−34	−64	46
Cuneus	L	19	16	3.52	0.006	−14	−84	32
Precuneus	L	31	25	3.29	0.012	−20	−72	31
Superior temporal gyrus	L	22	15	3.31	0.011	−48	−31	7
Right seed—inverse interaction								
No results								

BA: Brodmann area, L: left, R: right.

Although a few *p* values were below 0.05 in the expected direction (i.e. higher scores at retest in the actively treated group), none survived a statistical threshold corrected for multiple comparisons.

4. Discussion

We created a program of cognitive stimulation focused on the DMN, hypothesizing that it would up-regulate functional connectivity (a) within the posterior DMN and (b) between the anterior and posterior DMN sub-components. These two hypotheses were tested in a sample of healthy adults.

Construct validity of each task was verified in a two-fold manner: qualitatively, *a priori*, by the exploration of the neuropsychological literature and the identification of appropriate references supporting a connection between tasks and specific sets of brain areas, and *a posteriori*, by voxel-based correlational analyses carried out to characterize the pattern of GM maps associated with task performance. The patterns that emerged from these asso-

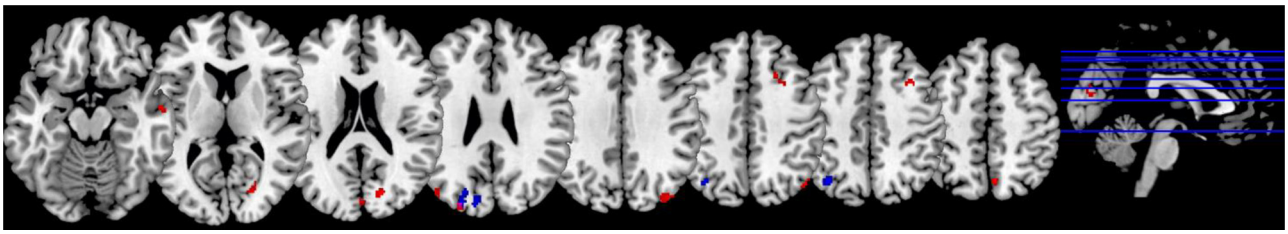

Fig. 4. Effect of the group-by-time-point interaction on seed based connectivity of the posterior cingulate. (For interpretation of the references to color in this figure legend, the reader is referred to the web version of this article)
Left posterior-cingulate connectivity is illustrated in red, whereas right posterior-cingulate connectivity is illustrated in blue. A significant (peak-level $pFWE < 0.05$) effect of the interaction was visible in midline and dorsal portions of the parietal lobe, bilaterally. Additional clusters (not all depicted in the figure) emerged in the occipital, temporal, frontal, and limbic lobe.
MNI coordinates of the slices are as follows: $z = -16, 10, 20, 28, 35, 43, 45, 50$.

Table 5
Analysis of seed-based connectivity of the posterior cingulate, increases and decreases as measured by within-sample *t* tests.

Brain region	Side	BA	Cluster size (voxels)	*Z* score at local maximum	D_{FWE} at peak level	Talairach coordinates		
						x	*y*	*z*
Experimental group								
Left seed increase								
Middle temporal gyrus	L	39	60	4.40	<0.001	−50	−69	16
Middle frontal gyrus	R	9	13	4.18	0.001	46	23	30
Precuneus	R	19	44	3.97	0.002	38	−68	38
Precuneus	R	39	21	3.09	0.026	46	−70	39
Precuneus	R	7	11	3.27	0.016	20	−73	46
Frontal sub-gyral	R	8	14	3.08	0.026	18	27	41
Left seed decrease								
Paracentral lobule	R	5	19	3.80	0.003	8	−44	59
Fusiform gyrus	L	37	31	3.29	0.015	−30	−43	−13
Right seed increase								
Angular gyrus	R	39	22	3.58	0.007	42	−62	34
Precuneus	R	7	16	3.47	0.009	22	−59	34
Superior occipital gyrus	L	19	14	3.17	0.021	−26	−76	26
Precuneus	L	31	19	3.17	0.022	−14	−49	30
Right seed decrease								
No results								
Control group								
Left seed increase								
No results								
Left seed decrease								
Middle frontal gyrus	R	8	22	3.98	0.002	30	16	40
Inferior parietal lobule	R	40	24	3.72	0.004	46	−64	44
Cuneus	L	18	32	3.63	0.006	−2	−71	13
Posterior cingulate	R	30	5	2.83	0.049	8	−68	9
Precuneus	R	7	16	3.49	0.009	6	−63	51
Superior parietal lobule	L	7	14	3.30	0.015	−32	−62	51
Cuneus	L	7	14	3.22	0.019	−18	−78	32
Right seed increase								
Middle cingulate gyrus	R	23	8	3.14	0.024	4	−24	33
Right seed decrease								
Middle frontal gyrus	L	8	42	3.78	0.004	−34	21	41
Posterior cingulate	R	31	19	3.46	0.010	18	−64	9
Middle temporal gyrus	R	37	20	3.28	0.016	48	−64	44
Superior parietal gyrus	L	7	32	3.18	0.021	−36	−64	47
Posterior cingulate	R	30	10	2.90	0.042	8	−69	9

BA: Brodmann area, L: left, R: right.

ciations covered mainly posterior areas of the neocortex, with GM correlates located in the hippocampal formation and in Brodmann areas 9, 21, 31, 39 and 40. These regions have been indicated as core regions associated with the DMN (Buckner et al., 2008). In addition, also precuneal GM emerged as a major correlate. An association with this set of areas was particularly visible for tasks focused on semantic retrieval and decisional speed. On the other hand, the overall association was weaker for tasks based on logical reasoning, with two tasks not showing any significant correlate. Although no consistent or qualitatively comparable pattern of association emerged between different tasks, this did not represent a substantial issue. Indeed, the experimental hypothesis implied an impact on functional connectivity of the entire program of stimulation as a single entity. For this reason the pattern of association was interpreted comprehensively. Tasks were designed *a priori* to achieve co-activation of posterior and prefrontal areas; however, an association between the program of stimulation and the anterior DMN emerged in prefrontal or anterolimbic clusters only in two tasks.

Table 6
Global volumetric measures at baseline and at the end of the study.

Structural measure	Experimental condition			Control condition			p_t test baseline group difference	p_{ANOVA} treatment effect
	Baseline	Retest	*n*	Baseline	Retest	*n*		
Vol_{GM}	573.48 (58.54)	576.29 (60.71)	21	603.15 (68.65)	601.96 (71.45)	19	0.148	0.115
Vol_{WM}	440.96 (39.20)	442.25 (37.12)	21	473.68 (66.76)	473.77 (67.46)	19	0.063	0.470
Vol_{CSF}	620.60 (81.76)	613.91 (80.42)	21	607.31 (110.98)	610.60 (112.99)	19	0.667	0.135
TIV	1635.04 (135.00)	1632.45 (130.42)	21	1684.14 (164.60)	1686.34 (159.82)	19	0.307	0.344
$Ratio_{GM}$	0.35 (0.02)	0.35 (0.02)	21	0.36 (0.03)	0.36 (0.03)	19	0.334	0.112
$Ratio_{WM}$	0.27 (0.02)	0.27 (0.02)	21	0.28 (0.03)	0.28 (0.03)	19	0.142	0.249
$Ratio_{GM+WM}$	0.62 (0.03)	0.62 (0.03)	21	0.64 (0.05)	0.64 (0.06)	19	0.184	0.112

Volumes are expressed in cm^3.

Table 7
Regional changes in GM and WM volumetric maps as measured by group-by-time-point interactions.

Brain region	Side	BA	Cluster size (voxels)	*Z* score at local maximum	D_{FWE} at peak level	Talairach coordinates		
						x	*y*	*z*
GM interaction								
Cerebellum—culmen	L		25	3.20	0.018	−30	−32	−20
Fusiform gyrus	L	20	15	3.01	0.030	−36	−40	−18
GM inverse interaction								
No results								
WM interaction								
No results								
WM inverse interaction								
No results								

BA: Brodmann area, L: left, R: right, GM: gray matter, WM: white matter.

Table 8
Regional changes in GM volumetric maps as measured by within-subject *t* tests.

Brain region	Side	BA	Cluster size (voxels)	*Z* score at local maximum	D_{FWE} at peak level	Talairach coordinates		
						x	*y*	*z*
Experimental group								
GM increase								
Cerebellum—culmen	L		32	3.90	0.002	−18	−38	−17
Fusiform gyrus	L	37	31	3.29	0.015	−34	−43	−13
Cerebellum—culmen	R		20	3.24	0.017	24	−36	−15
Superior parietal lobule	L	40	15	3.12	0.024	−36	−68	48
GM decrease								
No results								
Control group								
GM increase								
No results								
GM decrease								
Posterior cingulate	R	29	35	3.67	0.005	2	−42	19
Parahippocampal gyrus	R	30	27	3.37	0.012	18	−48	8
Posterior cingulate	R	30	6	2.94	0.036	24	−54	14

BA: Brodmann area, L: left, R: right, GM: gray matter, WM: white matter.

Changes in seed-based connectivity induced by the stimulation program showed a pattern of findings consistent with the outcome of the associational analysis. In fact, increased functional connectivity was found between the posterior cingulate and various clusters mainly located in temporal and parieto-occipital regions. These included the precuneus, the inferior parietal lobule, the temporal cortex and the parahippocampal gyrus, which, together with the posterior cingulate, are major computational stations included in the DMN. This piece of evidence was interpreted as up-regulation of posterior circuits within the DMN, and supported positively the first of the two experimental hypotheses. Aside from this set of areas, additional clusters showed increased connectivity with the seeds. These were located in the cuneus and in other parietal areas else than the inferior parietal lobule or the precuneus. These findings represent increases of connectivity outside the pathways of the DMN, but still within the DMN template. The use of a template was implemented in the analytical procedure to fit the directionality of the experimental hypothesis. Rather than using a "standard" DMN template based on the literature, however, a data-driven one was created based on the resting-state architecture of functional connectivity observed in our specific sample. This is a methodological strength, because the variables measured in the participants were confronted to a frame of reference obtained from the participants themselves. By doing so, a conservative approach was adopted, and the template turned out to be slightly larger than the classic set of areas normally described in the literature as DMN, especially in its parieto-occipital portion. For this reason, a larger pattern of changes in connectivity was found.

Limited evidence of increased connectivity was found between the seeds and prefrontal clusters. These frontal regions, albeit being

Fig. 5. Effect of the group-by-time-point interaction on GM volumes. (For interpretation of the references to color in this figure, the reader is referred to the web version of this article)
The interaction contrast revealed a sole significant cluster, located in the left cerebellar hemisphere (in proximity of lobules IV and V), and extending to the adjacent fusiform gyrus (most likely an artefactual finding, as the two regions are separated by the tentorium).
MNI coordinates of the slice is $z = -22$. GM: gray matter.

part of the DMN (as found, for example, by Damoiseaux et al. (2012)), were not located on the midline where the main anterior computational hub of the DMN is considered to be (i.e. Uddin et al., 2009). For this reason, maintaining again a conservative approach, we conclude that the second of the two experimental hypotheses is not sufficiently supported by these data. This finding, again, was consistent with the pattern of association from the correlational analyses. The persisting convergence between task correlates and areas showing increase after training is a strong piece of evidence supporting the validity of the stimulation program.

The findings of this investigation are of particular importance for the study of non-pharmacological therapeutics for early stage AD. In fact, AD causes a progressive down-regulation of brain function in the posterior areas of the cerebral cortex. This has been reported as a major finding in association with multiple neuroimaging and analytical procedures, such as, among others, the analysis of cerebral blood flow (Kogure et al., 2000), brain metabolism (Mosconi, 2005), regional homogeneity of BOLD signal (Zhang et al., 2012), functional connectivity of independent components measured with resting-state fMRI (Song et al., 2013) and, albeit being a measure only indirectly associated with brain function, Diffusion Tensor Imaging (Zhou et al., 2008). As a consequence, the observed pattern of association and the changes in the functional connectivity of the posterior cingulate that were obtained indicate that this stimulation program has the potential to trigger a beneficial impact on brain function in MCI or early AD patients. This has to be investigated in future studies designed *ad hoc*.

Volumetric changes in regional GM were also found. These included increased volumes in the experimental group in a portion of the left anterior cerebellum, which extended to part of the fusiform gyrus. Moreover, decrements were observed in mediotemporal-posterolimbic regions of those who had not been treated. It is interesting to note how the structural changes which emerged from the effect of the interaction were located in areas in which no change in connectivity was observed and, concurrently, no volumetric change was found in those regions where connectivity was up-regulated by the training. This structural-functional dissociation needs to be carefully examined, and appropriately interpreted. It has been suggested that changes in brain function can either be due to neuroplastic modifications of the structural substrate triggered by the training (which, in turn, cause functional change), or can be the simple consequence of a more flexible use of existing neural pathways, without any induced structural modification (Lövdén et al., 2010). Albeit both types of mechanism may have given their share of contribution to the findings, we suggest that the functional changes observed in this study were mainly the result of structural alterations. We had initially hypothesized that induced co-activation of multiple DMN regions would have translated into inter-regional regulation of resting-state functional connectivity of the DMN. Since the strength of functional connectivity between areas A and B depends strongly on the physical connections, in terms of direct and indirect pathways of structural connectivity between A and B (Damoiseaux and Greicius, 2009), it can be logically inferred that the mechanism we relied on to regulate functional connectivity was strongly based on a neuroplastic hypothesis, in which any regulation of functional connectivity is unavoidably associated with regulation of physical connections. As a consequence, some sort of meaningful structural changes must have sustained the modification of the observed pattern of functional connectivity. The absence of anatomical change in those regions where functional changes were observed is due, in all likelihood, to the "macroscopic" nature of VBM, which is unable to capture those fine-grained modification of brain tissue that may have been triggered by the cognitive stimulation program. When it comes to WM, Diffusion Tensor Imaging is extremely more sensitive than VBM in detecting both cross-sectional alterations (Hugenschmidt et al., 2008) as well as longitudinal modifications (Sagi et al., 2012) of fibres' diffusivity. For GM, on the other hand, VBM is capable of characterizing treatment effects as long as the biological nature of the morphological modification sustaining the functional change is sufficiently large to be visualized. At present, the exact biological mechanisms associated with cognitive stimulation which can alter GM and WM volumes in the human brain can only be speculated on, based on investigations carried out on animal models (Zatorre et al., 2012). We propose that in this study up-regulation of functional connectivity within regions included in the DMN was fostered by an increase in the number of regional synapses. It is thus suggested that the co-activation of multiple areas stimulated the development of new inter-cellular connections, which in turn resulted into increments of functional connectivity. This would also explain why no consistent VBM change was observed. Indeed, voxel size (the smallest unit of measurement included in the neuroimaging analyses) was around 1 mm^3, that is remarkably larger than the size of a single synapse, which generally ranges between 2 and 4×10^{-5} mm. If increased synaptic density were the main anatomical change sustaining functional increase, then it would be normal not to expect substantial macrostructural change as measured with VBM. We, therefore, acknowledge the absence of a sufficiently sensitive methodology to assess anatomical modifications as a potential limiting factor for a theoretical interpretation of the findings of this study. Previously published studies suggested a similar mechanism to account for treatment-dependent GM volume reduction. Pruning of redundant synapses was suggested as a potential biological mechanism underlying GM loss in young adults treated with a stimulation program based on tasks training processing speed (Takeuchi et al., 2011a) or working memory (Takeuchi et al., 2011b). Although regional change in synaptic density is believed to be the main hypothesis-driven correlate of the functional connectivity changes observed in this investigation, other types of

structural modifications or non-neuroplastic processes may have contributed to the functional regulation. A previous publication reported enhancement of WM integrity speculating an increase in myelination induced by working memory training (Takeuchi et al., 2010). In a second study another biological pathway was suggested to account for a positive regulation of cerebral blood flow and functional connectivity of the DMN following a training program consisting of strategy-based tasks. The authors argued that the training left a neural "footprint" on the resting-state signal of their participants. This footprint would conceptualize partly as an aggregation of neurotransmitter-specific receptors triggered in pathways localized within the areas stimulated by the tasks, and partly as an enhanced synthesis of intra-neuronal molecules necessary for synaptic transmission (Chapman et al., 2013). In summary, it is possible that multiple cellular and synaptic mechanisms might have contributed to connectivity increases associated with the stimulation and these might be reflected by the more distant regional anatomical changes observed in this study.

Changes in cognitive abilities were also explored, but no finding surviving correction for multiple comparisons was detected by the ANOVAs. Two main reasons may account for these non-significant results. First, the performance over a group of tests showed a baseline ceiling effect. This was evident at least for the Token Test, the copy of the Rey Figure and the number of errors made in the Stroop Test (see Table 2). Second, the "synergic mix" of a large number of neuropsychological tests and the use of the Bonferroni correction impacted drastically on the threshold of significance, which was reduced from 0.05 to 0.0031. The reason for choosing such an extensive neuropsychological battery was motivated by the necessity of a complete characterization of the group of participants. In fact, since the goal of this study was testing the efficacy of a possible therapeutic instrument for patients with AD-type neurodegeneration, it was deemed necessary to evaluate its effect as comprehensively as possible. On the other hand, as mentioned above, the use of the Bonferroni correction was motivated by a conservative approach, in order to maximize the chance of avoiding Type I errors in these exploratory analyses. The effect of the group-by-time-point interaction showed a trend of significance for the Raven Progressive Matrices and the Digit Span Backwards, and, for the Letter Fluency Test, the effect of the interaction almost approached statistical significance. The fact that, in all cases, the trend was in the expected direction suggests that the stimulation program might have a small beneficial effect in these cognitive domains in the presence of a central nervous system free from neurodegeneration. Plausibly, this small effect size might be larger in the presence of early-stage AD neurodegeneration, where ceiling effects are normally not seen.

This study is not free from limitations. Aside from the absence of a sensitive instrument to detect microstructural change in brain structure, a potential shortcoming in the experimental design of this study may be the different types of stimulation which experimental and control participants were exposed to. Both the experimental and the control group engaged in cognitively stimulating activities in the period spanning between the two assessment phases. The control group, however, did not formally receive a stimulation which was structured in computerized sessions. Although we acknowledge this technical feature as a methodological aspect which is open to improvement (see, for instance, Thomas and Baker (2013) for a detailed analysis of the importance of an appropriate control condition), we believe that it played a marginal role in our design since all participants assigned to the control condition adhered to a daily regime of stimulating activities based on intense social contact within the same setting as the experimental group. Moreover, it has also to be acknowledged that our findings show a strong directionality (i.e. abundant up-regulation and little or no down-regulation of connectivity), which cannot be explained in terms of casual confounding factors. It is really hard to postulate that a pattern of findings interpretable as an enhancement of functional connectivity within the DMN would have actually been caused by the impact of casual or secondary variables (e.g. the use of a computer). In fact, it is likely that chance and intervenient variables would have a more unstructured impact on brain function. If we had included an active control group (engaging in a "placebo cognitive stimulation") in our design, it is likely that a "placebo effect" due to intervenient variables would have triggered the most significant impact in those regions that have been reported as the most susceptible to stimulation of the placebo type, and these are mainly located in anterior regions, in prefrontal and antero-cingulate regions (Cavanna et al.,, 2007). In addition, all analyses were run conservatively, to infer up-regulations as well as down-regulations of brain connectivity. Nevertheless, the pattern of findings showed a strong directionality, and for this reason it appears reasonable to conclude that it is highly unlikely that our results may reflect either chance or other intervenient variables. Furthermore, despite the longitudinal design, no follow up was described, and therefore it is unknown whether these functional changes were long-lasting or quickly reversible.

5. Conclusion

In conclusion, we designed and tested a program of cognitive tasks based on the stimulation of the DMN through the repeatedly induced co-activation of its computational hubs. Healthy participants showed functional regulation of resting-state connectivity within the posterior component of the DMN but no change in connectivity between the posterior and the anterior components. These findings suggest that the program devised may have a preventive and therapeutic role in association with early AD-type neurodegeneration.

Acknowledgements

We thank Luciano Foscolo, Francesco Spigariol and Valentina Citton for their help in the neuroradiological assessment of MRI scans. We also thank Luca Ghezzo, Elisa Duse and Antonio Tumbarello for their help in MRI data collection. This study was partially supported by grant no 42/RF-2010-2321718 by the Italian Ministry of Health and partial funding from the European Union Seventh Framework Program (FP7/2007-2013) under grant agreement no. 601055, VPH-DARE@IT to AV.

References

Ahmed, S., Arnold, R., Thompson, S.A., Graham, K.S., Hodges, J.R., 2008. Naming of objects, faces and buildings in mild cognitive impairment. Cortex 44 (6), 746–752, http://dx.doi.org/10.1016/j.cortex.2007.02.002.

Andrews-Hanna, J.R., Reidler, J.S., Sepulcre, J., Poulin, R., Buckner, R.L., 2010. Functional-anatomic fractionation of the brain's default mode network. Neuron 65 (4), 550–562, http://dx.doi.org/10.1016/j.neuron.2010.02.005.

Basso, A., Capitani, E., Laiacona, M., 1987. Raven's coloured progressive matrices: normative values on 305 adult normal controls. Funct. Neurol. 2 (2), 189–194.

Binder, J.R., Frost, J.A., Hammeke, T.A., Bellgowan, P.S., Rao, S.M., Cox, R.W., 1999. Conceptual processing during the conscious resting state. A functional MRI study. J. Cogn. Neurosci. 11 (1), 80–93, http://dx.doi.org/10.1162/089892999563265.

Binder, J.R., Desai, R.H., Graves, W.W., Conant, L.L., 2009. Where is the semantic system? A critical review and meta-analysis of 120 functional neuroimaging studies. Cereb. Cortex 19 (12), 2767–2796, http://dx.doi.org/10.1093/cercor/bhp055.

Bozzali, M., Dowling, C., Serra, L., Spanò, B., Torso, M., Marra, C., Castelli, D., Dowell, N.G., Koch, G., Caltagirone, C., Cercignani, M., 2015. The impact of cognitive reserve on brain functional connectivity in Alzheimer's disease. J. Alzheimers Dis. 14 (1), 243–250, http://dx.doi.org/10.3233/JAD-141824.

Brett, M., Anton, J.L., Valabregue, R., Poline, J.B., 2002. Region of interest analysis using an SPM toolbox [abstract]. In: Presented at the 8th International Conference of Functional Mapping of the Human Brain, June 2-6, 2002, Sendai, Japan, Available on CD-ROM in NeuroImage 16(2). 10.1016/S1053-8119(02)90013-3.

Buckner, R.L., Carroll, D.C., 2007. Self-projection and the brain. Trends Cogn. Sci. 11 (2), 49–57, http://dx.doi.org/10.1016/j.tics.2006.11.004.
Buckner, R.L., Andrews-Hanna, J.R., Schacter, D.L., 2008. The brain's default network. Anatomy, function, and relevance to disease. Ann. N. Y. Acad. Sci. 1124, 1–38, http://dx.doi.org/10.1196/annals.1440.011.
Caffarra, P., Vezzadini, G., Dieci, F., Zonato, F., Venneri, A., 2002a. Rey-Osterrieth complex figure: normative values in an Italian population sample. Neurol. Sci. 22 (6), 443–447.
Caffarra, P., Vezzadini, G., Dieci, F., Zonato, F., Venneri, A., 2002b. Una versione abbreviata del test di Stroop: dati normativi nella popolazione italiana. Nuova Riv. Neurol. 12 (4), 111–115.
Calhoun, V.D., Adali, T., Pearlson, G.D., Pekar, J.J., 2001. A method for making group inferences from functional MRI data using independent component analysis. Hum. Brain Mapp. 14 (3), 140–151, http://dx.doi.org/10.1002/hbm.1048.
Cavanna, A., Strigaro, G., Monaco, F., 2007. Brain mechanisms underlying the placebo effect in neurological disorders. Funct. Neurol. 22 (2), 89–94.
Chapman, S.B., Aslan, S., Spence, J.S., Hart Jr., J.J., Bartz, E.K., Didehbani, N., Keebler, M.W., Gardner, C.M., Strain, J.F., Defina, L.F., Lu, H.Z., 2015. Neural mechanisms of brain plasticity with complex training in healthy seniors. Cereb. Cortex 25 (2), 396–405, http://dx.doi.org/10.1093/cercor/bht234.
Cheng, C.M., Chiu, M.J., Wang, J.H., Liu, H.C., Shyu, Y.I.L., Huang, G.H., Chen, C.C.H., 2012. Cognitive stimulation during hospitalization improves global cognition of older Taiwanese undergoing elective total knee and hip replacement surgery. J. Adv. Nurs. 68 (6), 1322–1329, http://dx.doi.org/10.1111/j.1365-2648.2011.05842.x.
Damoiseaux, J.S., Greicius, M.D., 2009. Greater than the sum of its parts: A review of studies combining structural connectivity and resting-state functional connectivity. Brain Struct. Funct. 213 (6), 525–533, http://dx.doi.org/10.1007/s00429-009-0208-6.
Damoiseaux, J.S., Prater, K.E., Miller, B.L., Greicius, M.D., 2012. Functional connectivity tracks clinical deterioration in Alzheimer's disease. Neurobiol. Aging 33 (4), 828.e19–828.e30, http://dx.doi.org/10.1016/j.neurobiolaging.2011.06.024.
De Marco, M., Shanks, M.F., Venneri, A., 2014. Cognitive Stimulation: the evidence base for its application in neurodegenerative disease. Curr. Alzheimer Res. 11 (5), 469–483, http://dx.doi.org/10.2174/1567205011666140505120145.
Fangmeier, T., Knauff, M., Ruff, C.C., Sloutsky, V.M., 2006. fMRI evidence for a three-stage model of deductive reasoning. J. Cogn. Neurosci. 18 (3), 320–334.
Fouquet, M., Desgranges, B., Landeau, B., Duchesnay, E., Mézenge, F., de la Sayette, V., Viader, F., Baron, J.C., Eustache, F., Chételat, G., 2009. Longitudinal brain metabolic changes from amnestic mild cognitive impairment to Alzheimers disease. Brain 132 (pt 8), 2058–2067, http://dx.doi.org/10.1093/Brain/Awp132.
Fox, M.D., Raichle, M.E., 2007. Spontaneous fluctuations in brain activity observed with functional magnetic resonance imaging. Nat. Rev. Neurosci. 8 (9), 700–711, http://dx.doi.org/10.1038/nrn2201.
Franco, A.R., Pritchard, A., Calhoun, V.D., Mayer, A.R., 2009. Interrater and intermethod reliability of default mode network selection. Hum. Brain Mapp. 30 (7), 2293–2303, http://dx.doi.org/10.1002/hbm.20668.
Greicius, M.D., Krasnow, B., Reiss, A.L., Menon, V., 2003. Functional connectivity in the resting brain: a network analysis of the default mode hypothesis. Proc. Natl. Acad. Sci. U. S. A. 100 (1), 253–258, http://dx.doi.org/10.1073/pnas.0135058100.
Habas, C., Kamdar, N., Nguyen, D., Keller, K., Beckmann, C.F., Menon, V., Greicius, M.D., 2009. Distinct cerebellar contributions to intrinsic connectivity networks. J. Neurosci. 29 (26), 8586–8594, http://dx.doi.org/10.1523/jneurosci.1868-09.2009.
Hampel, H., Prvulovic, D., Teipel, S.J., Bokde, A.L.W., 2011. Recent development of functional magnetic resonance imaging research for drug development in Alzheimer's disease. Prog. Neurobiol. 95 (4), 570–578, http://dx.doi.org/10.1016/j.pneurobio.2011.05.012.
Han, S.D., Arfanakis, K., Fleischman, D.A., Leurgans, S.E., Tuminello, E.R., Edmonds, E.C., Bennett, D.A., 2012. Functional connectivity variations in mild cognitive impairment: associations with cognitive function. J. Int. Neuropsychol. Soc. 18 (1), 39–48, http://dx.doi.org/10.1017/s1355617711001299.
Harrison, B.J., Pujol, J., Ortiz, H., Fornito, A., Pantelis, C., Yücel, M., 2008. Modulation of brain resting-state networks by sad mood induction. PLoS One 3 (3), e1794, http://dx.doi.org/10.1371/journal.pone.0001794.
Hugenschmidt, C.E., Peiffer, A.M., Kraft, R.A., Casanova, R., Deibler, A.R., Burdette, J.H., Maldjian, J.A., Laurienti, P.J., 2008. Relating imaging indices of white matter integrity and volume in heathy older adults. Cereb. Cortex 18 (2), 433–442, http://dx.doi.org/10.1093/cercor/bhm080.
Jolles, D.D., van Buchem, M.A., Crone, E.A., Rombouts, S.A.R.B., 2013. Functional brain connectivity at rest changes after working memory training. Hum. Brain Mapp. 34 (2), 396–406, http://dx.doi.org/10.1002/hbm.21444.
Jones, D.T., Machulda, M.M., Vemuri, P., McDade, E.M., Zeng, G., Senjem, M.L., Gunter, J.L., Przybelski, S.A., Avula, R.T., Knopman, D.S., Boeve, B.F., Petersen, R.C., Jack Jr., C.R., 2011. Age-related changes in the default mode network are more advanced in Alzheimer disease. Neurology 77 (16), 1524–1531, http://dx.doi.org/10.1212/wnl.0b013e318233b33d.
Juncos-Rabadán, O., Rodríguez, N., Facal, D., Cuba, J., Pereiro, A.X., 2011. Tip-of-the-tongue for proper names in mild cognitive impairment. Semantic or post-semantic impairments? J. Neurolinguist. 24 (6), 636–651, http://dx.doi.org/10.1016/j.jneuroling.2011.06.004.
Koch, W., Teipel, S., Müller, S., Bürger, K., Bokde, A.L.W., Hampel, H., Coates, U., Reiser, M., Meindl, T., 2010. Effects of aging on default mode network activity in resting state fMRI: does the method of analysis matter? Neuroimage 51 (1), 280–287, http://dx.doi.org/10.1016/j.neuroimage.2009.12.008.
Kogure, D., Matsuda, H., Ohnishi, T., Asada, T., Uno, M., Kunihiro, T., Nakano, S., Takasaki, M., 2000. Longitudinal evaluation of early Alzheimer's disease using brain perfusion SPECT. J. Nucl. Med. 41 (7), 1155–1162.
Lorenzi, M., Beltramello, A., Mercuri, N.B., Canu, E., Zoccatelli, G., Pizzini, F.B., Alessandrini, F., Cotelli, M., Rosini, S., Costardi, D., Caltagirone, C., Frisoni, G.B., 2011. Effect of memantine on resting state default mode network activity in Alzheimer's disease. Drugs Aging 28 (3), 205–217, http://dx.doi.org/10.2165/11586440-000000000-00000.
Lövdén, M., Bäckman, L., Lindenberger, U., Schaefer, S., Schmiedek, F., 2010. A theoretical framework for the study of adult cognitive plasticity. Psychol. Bull. 136 (4), 659–676, http://dx.doi.org/10.1037/a0020080.
Machulda, M.M., Jones, D.T., Vemuri, P., McDade, E., Avula, R., Przybelski, S., Boeve, B.F., Knopman, D.S., Petersen, R.C., Jack Jr., C.R., 2011. Effect of APOE ε 4 status on intrinsic network connectivity in cognitively normal elderly subjects. Arch. Neurol. 68 (9), 1131–1136, http://dx.doi.org/10.1001/archneurol.2011.108.
Martínez, K., Solana, A.B., Burgaleta, M., Hernández-Tamames, J.A., Álvarez-Linera, J., Román, F.J., Alfayate, E., Privado, J., Escorial, S., Quiroga, M.A., Karama, S., Bellec, P., Colom, R., 2013. Changes in resting-state functionally connected parietofrontal networks after videogame practice. Hum. Brain Mapp. 34 (12), 3143–3157, http://dx.doi.org/10.1002/hbm.22129.
Mevel, K., Landeau, B., Fouquet, M., La Joie, R., Villain, N., Mézenge, F., Perrotin, A., Eustache, F., Desgranges, B., Chételat, G., 2013. Age effect on the default mode network, inner thoughts, and cognitive abilities. Neurobiol. Aging 34 (4), 1292–1301, http://dx.doi.org/10.1016/j.neurobiolaging.2012.08.018.
Mosconi, L., 2005. Brain glucose metabolism in the early and specific diagnosis of Alzheimer's disease: FDG-PET studies in MCI and AD. Eur. J. Nucl. Med. Mol. Imaging 32 (4), 486–510, http://dx.doi.org/10.1007/s00259-005-1762-7.
Mowinckel, A.M., Espeseth, T., Westlye, L.T., 2012. Network-specific effects of age and in-scanner subject motion: a resting-state fMRI study of 238 healthy adults. Neuroimage 63 (3), 1364–1373, http://dx.doi.org/10.1016/j.neuroimage.2012.08.004.
Novelli, A., Papagno, C., Capitani, E., Laiacona, N., Vallar, G., Cappa, S.F., 1986a. Tre test clinici di memoria verbale a lungo termine. Arch. Psicol. Neurol. Psichiatr. 47 (2), 278–296.
Novelli, A., Papagno, C., Capitani, E., Laiacona, N., Vallar, G., Cappa, S.F., 1986b. Tre test clinici di ricerca e produzione lessicale. Taratura su soggetti normali. Arch. Psicol. Neurol. Psichiatr. 47 (4), 477–506.
Orsini, A., Grossi, D., Capitani, E., Laiacona, M., Papagno, C., Vallar, G., 1987. Verbal and spatial immediate memory span—normative data from 1355 adults and 1112 children. Ital. J. Neurol. Sci. 8 (6), 539–548.
Osterrieth, P.A., 1944. Le test de copie d'une figure complexe. Arch. Psychol. 30, 206–356.
Raichle, M.E., MacLeod, A.M., Snyder, A.Z., Powers, W.J., Gusnard, D.A., Shulman, G.L., 2001. A default mode of brain function. Proc. Natl. Acad. Sci. U. S. A. 98 (2), 676–682, http://dx.doi.org/10.1073/pnas.98.2.676.
Raven, J.C., 1947. Progressive Matrices: Sets A, AB, and B. Seine, Clamart.
Rey, A., 1941. L'examen psychologique dans les cas d'encéphalopathie traumatic. Arch. Psycholo. 28, 286–340.
Rosazza, C., Minati, L., Ghielmetti, F., Mandelli, M.L., Bruzzone, M.G., 2012. Functional connectivity during resting-state functional MR imaging: study of the correspondence between independent component analysis and region-of-interest-based methods. Am. J. Neuroradiol. 33 (1), 180–187, http://dx.doi.org/10.3174/ajnr.a2733.
Rypma, B., Berger, J.S., Prabhakaran, V., Bly, B.M., Kimberg, D.Y., Biswal, B.B., D'Esposito, M., 2006. Neural correlates of cognitive efficiency. Neuroimage 33 (3), 969–979, http://dx.doi.org/10.1016/j.neuroimage.2006.05.065.
Sagi, Y., Tavor, I., Hofstetter, S., Tzur-Moryosef, S., Blumenfeld-Katzir, T., Assaf, Y., 2012. Learning in the fast lane: new insights into neuroplasticity. Neuron 73 (6), 1195–1203, http://dx.doi.org/10.1016/j.neuron.2012.01.025.
Santz-Arigita, E.J., Schoonheim, M.M., Damoiseaux, J.S., Rombouts, S.A.R.B., Maris, E., Barkhof, F., Scheltens, P., Stam, C.J., 2010. Loss of 'small-world' networks in Alzheimer's disease: graph analysis of fMRI resting-state functional connectivity. PLoS One 5 (11), e13788, http://dx.doi.org/10.1371/journal.pone.0013788.
Snodgrass, J.G., Vanderwart, M.S., 1980. Sandardized set of 260 pictures—norms for name agreement, image agreement, familiarity, and visual complexity. J. Exp. Psychol.: Hum. Learn. Mem. 6 (2), 174–215.
Solé-Padullés, C., Bartrés-Faz, D., Lladó, A., Bosch, B., Peña-Gómez, C., Castellví, M., Rami, L., Bargalló, N., Sánchez-Valle, R., Molinuevo, J.L., 2013. Donepezil treatment stabilizes functional connectivity during resting state and brain activity during memory encoding in Alzheimer's disease. J. Clin. Psychopharmacol. 33 (2), 199–205, http://dx.doi.org/10.1097/JCP.0b013e3182825bfd.
Song, J.Y., Qin, W., Liu, Y., Duan, Y.Y., Liu, J.Q., He, X.X., Li, K.C., Zhang, X.Q., Jiang, T.Z., Yu, C.S., 2013. Aberrant functional organization within and between resting-state networks in AD. PLoS One 8 (5), e63727, http://dx.doi.org/10.1371/journal.pone.0063727.
Song, X.W., Dong, Z.Y., Long, X.Y., Li, S.F., Zuo, X.N., Zhu, C.Z., He, Y., Yan, C.G., Zang, Y.F., 2011. REST: a toolkit for resting-state functional magnetic resonance imaging data processing. PLoS One 6 (9), e25031, http://dx.doi.org/10.1371/journal.pone.0025031.
Spinnler, H., Tognoni, G., 1987. Standardizzazione e taratura italiana di test neuropsicologici. Ital. J. Neurol. Sci. 6 (Suppl. 8), 1–120.

Stroop, J.R., 1935. Studies of interference in serial verbal reactions. J. Exp. Psychol. 18 (6), 643–662.
Takeuchi, H., Sekiguchi, A., Taki, Y., Yokoyama, S., Yomogida, Y., Komuro, N., Yamanouchi, T., Suzuki, S., Kawashima, R., 2010. Training of working memory impacts structural connectivity. J. Neurosci. 30 (9), 3297–3303, http://dx.doi.org/10.1523/jneurosci.4611-09.2010.
Takeuchi, H., Taki, Y., Hashizume, H., Sassa, Y., Nagase, T., Nouchi, R., Kawashima, R., 2011a. Effects of training of processing speed on neural systems. J. Neurosci. 31 (34), 12139–12148, http://dx.doi.org/10.1523/jneurosci.2948-11.2011.
Takeuchi, H., Taki, Y., Sassa, Y., Hashizume, H., Sekiguchi, A., Fukushima, A., Kawashima, R., 2011b. Working memory training using mental calculation impacts regional gray matter of the frontal and parietal regions. PLoS One 6 (8), e23175, http://dx.doi.org/10.1371/journal.pone.0023175.
Thomas, C., Baker, C.I., 2013. Teaching an adult brain new tricks: a critical review of evidence for training-dependent structural plasticity in humans. Neuroimage 73, 225–236, http://dx.doi.org/10.1016/j.neuroimage.2012.03.069.
Tyler, L.K., Marslen-Wilson, W., Stamatakis, E.A., 2005. Dissociating neuro-cognitive component processes: voxel-based correlational methodology. Neuropsychologia 43 (5), 771–778, http://dx.doi.org/10.1016/j.neuropsychologia.2004.07.020.
Uddin, L.Q., Kelly, A.M.C., Biswal, B.B., Castellanos, F.X., Milham, M.P., 2009. Functional connectivity of default mode network components: correlation, anticorrelation, and causality. Hum. Brain Mapp. 30 (2), 625–637, http://dx.doi.org/10.1002/hbm.20531.
Utevsky, A.V., Smith, D.V., Huettel, S.A., 2014. Precuneus is a functional core of the default-mode network. J. Neurosci. 34 (3), 932–940, http://dx.doi.org/10.1523/jneurosci.4227-13.2014.
Venneri, A., Molinari, M.A., Pentore, R., Cotticelli, B., Nichelli, P., Caffarra, P., 1993. Shortened stroop color-word test: its application in Alzheimer's disease. In: Nicolini, M., Zatta, P.F., Corain, B. (Eds.), Alzheimer's disease and related disorders. Pergamon Press, Great Britain, pp. 81–82.
Voss, M.W., Prakash, R.S., Erickson, K.I., Boot, W.R., Basak, C., Neider, M.B., Simons, D.J., Fabiani, M., Gratton, G., Kramer, A.F., 2012. Effects of training strategies implemented in a complex videogame on functional connectivity of attentional networks. Neuroimage 59 (1), 138–148, http://dx.doi.org/10.1016/j.neuroimage.2011.03.052.
Wang, K., Liang, M., Wang, L., Tian, L.X., Zhang, Z.Q., Li, K.C., Jiang, T.Z., 2007. Altered functional connectivity in early Alzheimer's disease: a resting-state fMRI study. Hum. Brain Mapp. 28 (10), 967–978, http://dx.doi.org/10.1002/hbm.20324.
Wechsler, D., 1981. WAIS-R Manual. The Psychological Corporation, New York.
Whitlock, L.A., McLaughlin, A.C., Allaire, J.C., 2012. Individual differences in response to cognitive training: using a multi-modal, attentionally demanding game-based intervention for older adults. Comput. Hum. Behav. 28 (4), 1091–1096, http://dx.doi.org/10.1016/j.chb.2012.01.012.
Wirth, M., Jann, K., Dierks, T., Federspiel, A., Wiest, R., Horn, H., 2011. Semantic memory involvement in the default mode network: a functional neuroimaging study using independent component analysis. Neuroimage 54 (4), 3057–3066, http://dx.doi.org/10.1016/j.neuroimage.2010.10.039.
Wu, J.T., Wu, H.Z., Yan, C.G., Chen, W.Y., Zhang, H.Y., He, Y., Yang, H.S., 2011. Aging-related changes in the default mode network and its anti-correlated networks: a resting-state fMRI study. Neurosci. Lett. 504 (1), 62–67, http://dx.doi.org/10.1016/j.neulet.2011.08.059.
Yasuda, K., Nakamura, T., Beckman, B., 2000. Brain processing of proper names. Aphasiology 14 (11), 1067–1089, http://dx.doi.org/10.1080/02687030050174638.
Zatorre, R.J., Fields, R.D., Johansen-Berg, H., 2012. Plasticity in gray and white: neuroimaging changes in brain structure during learning. Nat. Neurosci. 15 (4), 528–536, http://dx.doi.org/10.1038/nn.3045.
Zhang, Z.Q., Liu, Y., Jiang, T.Z., Zhou, B., An, N.Y., Dai, H.T., Wang, P., Liu, Y.X., Wang, L.N., Zhang, X., 2012. Altered spontaneous activity in Alzheimer's disease and mild cognitive impairment revealed by regional homogeneity. Neuroimage 59 (2), 1429–1440, http://dx.doi.org/10.1016/j.neuroimage.2011.08.049.
Zhou, Y.X., Dougherty Jr., J.H., Hubner, K.F., Bai, B., Cannon, R.L., Hutson, R.K., 2008. Abnormal connectivity in the posterior cingulate and hippocampus in early Alzheimer's disease and mild cognitive impairment. Alzheimers Dement. 4 (4), 265–270, http://dx.doi.org/10.1016/j.jalz.2008.04.006.